RSC Advances

PAPER

View Article Online
View Journal | View Issue

Cite this: *RSC Adv.*, 2023, **13**, 9642

A green method for decolorization of polysaccharides from alfalfa by S-8 macroporous resin and their characterization and antioxidant activity

Xiaohong Yu, Na Mu, Xiaochen Liu, Yueling Shang, Dujun Wang and Fengwei Li *

In this study, the decolorization conditions of polysaccharides extracted from alfalfa by S-8 macroporous adsorption resin were optimized through the response surface method, and the physicochemical properties and antioxidant activity of decolorized polysaccharides were investigated. The optimal decolorization conditions were determined to be as follows: the amount of S-8 macroporous adsorption resin was 1.4 g, the adsorption time was 2 h, and the adsorption temperature was 58 °C. Under these optimal conditions, a decolorization ratio of 71.43 ± 0.23% was achieved, which was consistent with the model hypothesis. The adsorption curve showed that S-8 macroporous adsorption resin adsorption of pigment molecules in alfalfa polysaccharides (APS) agreed with the Freundlich and pseudo-second-order equations, and the adsorption was a spontaneous endothermic process. High-performance liquid chromatography (HPLC) analysis of monosaccharide composition showed that APS was composed of mannose, glucose, galactose, arabinose and glucuronic acid in a molar ratio of 1.18 : 8.04 : 1.22 : 0.92 : 1. The results of antioxidant activity studies showed that APS had strong scavenging activity against ABTS, DPPH and hydroxyl radicals. This study will help to further understand the adsorption mechanism of macroporous resin on polysaccharide pigment molecules and lay a basis for evaluating their physiological activity.

Received 4th February 2023
Accepted 16th March 2023

DOI: 10.1039/d3ra00756a

rsc.li/rsc-advances

1. Introduction

Alfalfa (*Medicago sativa* L.), a perennial herb belonging to the genus *Medicago* under the Fabaceae family, is widely cultivated around the world due to its high feeding and edible value.[1] Alfalfa has been used as a medicinal plant for centuries, as it contains abundant bioactive ingredients, such as polysaccharides, flavonoids, and saponins. Polysaccharides are among its main active components and have been found to have a variety of physiological activities, such as neuroprotection,[2] antioxidation,[3] immunomodulation and regulation of intestinal microecology.[4,5] In recent decades, plant-derived polysaccharides have been widely used in different fields, such as food, medicine and cosmetics, due to their broad efficacy and low toxicity.[6] However, when preparing polysaccharides, coexisting pigments may be found, which may affect their structural characterization and biological activity analysis, and increase difficulties for further research of polysaccharides,[7] and no relevant studies on alfalfa polysaccharides (APS) decolorization have been conducted. Therefore, decolorization plays an important role in studying the APS.

At present, many polysaccharides decolorization methods, such as activated carbon adsorption, macroporous resin adsorption and H_2O_2 oxidation, have been reported.[8] Various methods have different mechanisms of action. H_2O_2 depends on its strong oxidation ability to achieve decolorization. However, it may destroy the structure and some functional groups of polysaccharides, which in turn impact their biological activity.[9] Activated carbon decolorization is a type of physical decolorization; under the action of van der Waals forces and electrostatic forces, pigment molecules are fixed in the porous structure of activated carbon.[10] However, this method is time-consuming, and the selectivity of activated carbon to polysaccharides is low, leading to an increase in the loss rate of polysaccharides.[11] Macroporous resin adsorption is a physical adsorption method with the advantages of a good adsorption effect on pigments, a low polysaccharides loss rate, simple operation, and so on, thus it is a suitable method for polysaccharides decolorization.[12] The pigment molecules in the polysaccharides solution were adsorbed by macroporous resin, which can largely remove the pigment impurities in polysaccharides without affecting the characteristic groups and molecular weight of polysaccharides. The method is superior to H_2O_2 oxidation and activated carbon adsorption methods.[11] S-8 macroporous adsorption resin is a polar adsorbent with

School of Marine and Bioengineering, Yancheng Institute of Technology, Yancheng 224051, China. E-mail: lifengwei1980@126.com

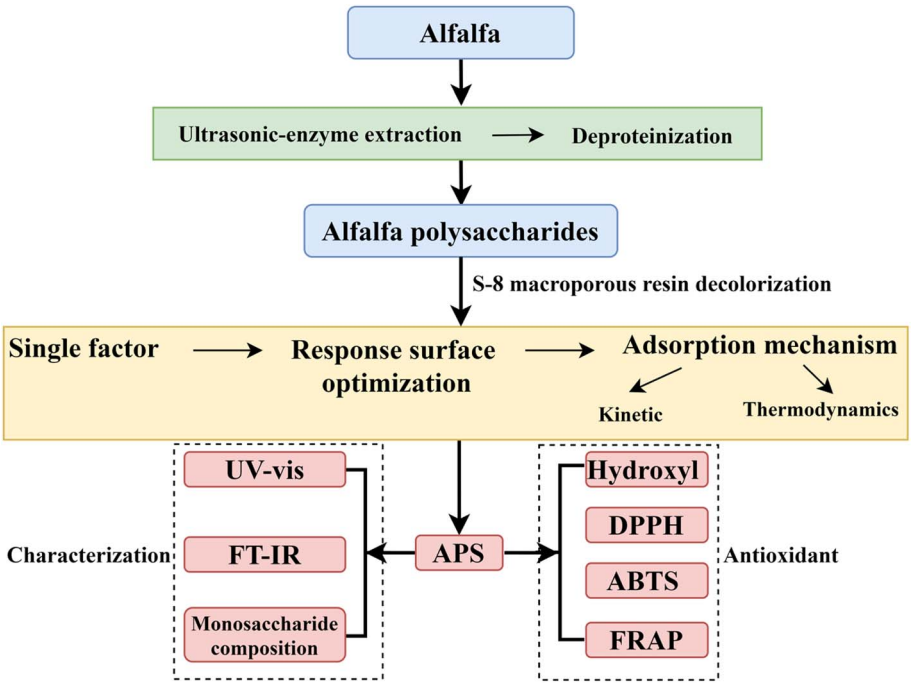

Fig. 1 The flow chart of experimental design.

diethylenebenzene as the backbone structure, which has strong adsorption ability for some molecules with similar properties, and its physical and chemical properties are stable, so it can be used to remove the medium-polar and polar pigment molecules from polysaccharides.

Many organisms produce energy through the oxidation process. However, if the oxidation reaction produces excessive reactive oxygen species, it will lead to the occurrence of some chronic diseases. Therefore, the development and utilization of safe and effective antioxidants to reduce the invasion of diseases have attracted extensive attention. Recently, polysaccharides have emerged as potential sources of new antioxidants because of their relatively low toxicity and strong antioxidant activity. Studies have shown that many natural polysaccharides can effectively prevent oxidative damage to organisms as free radical scavengers. APS is expected to become potential natural antioxidants due to its abundant sources and special biological functions.[13–15] To date, there is limited information on the antioxidant activity of APS extracted by the ultrasonic-enzyme method and decolorized by S-8 macroporous adsorption resin.

Accordingly, in this study, the decolorization process of static adsorption of pigment molecules in APS by S-8 macroporous adsorption resin was optimized by single factor and response surface method to improve the purity of APS and be beneficial to the structural analysis and biological activity research. Then the adsorption kinetics and thermodynamics models were studied to clarify the mechanism of adsorption of pigment molecules in APS by macroporous resin. Finally, its conformation and monosaccharide composition were determined by high-performance liquid chromatography (HPLC), ultraviolet-visible (UV-vis) spectrum and Fourier-transform infrared (FT-IR) spectroscopy. In addition, the antioxidant activity of APS *in vitro* was investigated, which provided a theoretical basis for its development as antioxidants and its application in functional foods. The flow chart of experimental design is shown in Fig. 1.

2. Materials and methods

2.1 Materials and chemicals

Alfalfa was obtained from Cangzhou City, Hebei Province. A specimen with voucher No. MSL2021 was deposited at the School of Marine and Bioengineering, Yancheng Institute of Technology. Cellulase (50 U mg^{-1}), papain (800 U mg^{-1}), pectinase (500 U mg^{-1}), S-8 macroporous adsorption resin, monosaccharide standards, vitamin C (Vc), 2,2′-azino-bis-(3-ethylbenzothiazoline-6-sulfonic acid) (ABTS) and 2,2-diphenyl-1-picrylhydroxyl (DPPH) were provided by Shanghai Yuanye Bio-Technology Co., Ltd. (Shanghai, China). The other reagents were analytically pure.

2.2 Extraction of APS

Alfalfa stems and leaves were dried at 55 °C for 48 h, pulverized in a 40-mesh sieve, and stored for later use. The alfalfa powder was degreased and decolorized by refluxing with petroleum ether in a Soxhlet extractor for 60 h. The residue was ventilated to evaporate the residual solvent and dried in an oven at 55 °C for 24 h. APS was extracted by an ultrasonic-enzyme assisted method based on published literature with minor modifications.[3] Briefly, the sample was mixed with deionized water at a ratio of 1 : 30, and cellulase, pectinase and papain with total

enzyme amounts of 1% were added (enzyme activity = 1 : 1 : 1). After mixing, the mixture was sonicated at 50 °C for 50 min, and then the reaction temperature was quickly increased to 95 °C for 10 min to inactivate the enzyme. The supernatant was collected and concentrated at 50 °C in vacuum to reduce the volume, and then added 4 times volume of anhydrous ethanol and precipitated for 24 h. Proteins were removed from the polysaccharides using the Sevag method.[16] Finally, heteropolysaccharides was obtained after freeze-drying.[17]

2.3 APS decolorization by S-8 macroporous adsorption resin

2.3.1 Single factor test. The effects of the amount of S-8 macroporous adsorption resin (0.5, 1.0, 1.5, 2.0 and 2.5 g), adsorption time (0.5, 1, 1.5, 2 and 2.5 h), polysaccharides concentration (4, 6, 8, 10 and 12 mg mL^{-1}) and adsorption temperature (30, 40, 50, 60 and 70 °C) on the decolorization of polysaccharides were determined by single-factor experiments. The results of each condition were analysed by the decolorization ratio and polysaccharides retention ratio.

The absorbance values of the original and decolorized polysaccharides solution were measured at 420 nm,[7] and the decolorization ratio was calculated according to eqn (1).

$$\text{Decolorization ratio } (\%) = \frac{A_1 - A_2}{A_1} \times 100 \quad (1)$$

where A_1 and A_2 are the absorbance values before and after decolorization, respectively.

The polysaccharides retention ratio was determined by the phenol sulfate method and calculated according to eqn (2).[18]

$$\text{Polysaccharides retention ratio } (\%) = \frac{A_3}{A_4} \times 100 \quad (2)$$

where A_4 and A_3 represent the absorbance values before and after decolorization, respectively.

2.3.2 Optimization decolorization conditions. Based on the single-factor test, the Box–Behnken design was used to carry out response surface optimization experiments with the amount of resin (A), adsorption time (B) and adsorption temperature (C) as independent variables and the decolorization ratio as the dependent variable. The independent variables were represented by −1, 0 and 1 (as shown in Table 1).

2.4 Adsorption studies

2.4.1 Adsorption kinetic studies. Ten grams of resin was mixed with 50 mL (10 mg mL^{-1}) of APS solution and left for 150 min at 20, 30 and 40 °C. Samples were collected at 10 min intervals, and the absorbance values were measured at 420 nm by means of a Multiskan SkyHigh plate-reader (Thermo Fisher, USA).

2.4.2 Adsorption thermodynamic studies. Different amounts of resin (6, 7, 8, 9, 10, and 11 g) were fixed with 50 mL (10 mg mL^{-1}) of APS solution and were adsorbed at 20, 30, and 40 °C for 150 min. Then, the absorbance values of the APS solution were tested at 420 nm.

Table 1 The independent variables and their levels employed in the Box–Behnken design

			Level of factors		
Factors	Unit	Code	−1	0	1
Amount of resin	g	A	1	1.5	2
Adsorption time	h	B	1.5	2	2.5
Adsorption temperature	°C	C	50	60	70

2.5 Characterization of APS after decolorization

2.5.1 Analysis of UV-vis and FT-IR. The UV-vis spectra of APS (1.0 mg mL^{-1}) in the range of 200–800 nm were measured with a Multiskan SkyHigh Plate reader, and the FT-IR spectra of APS (3 mg) in the range of 4000–400 cm^{-1} were obtained on an FT-IR spectrometer with a resolution of <0.09 cm^{-1} (Nicolet iS10, Thermo Fisher, USA).

2.5.2 Analysis of the monosaccharide composition. The monosaccharide composition of APS was determined by HPLC (LC1260, Agilent, USA) using 1-phenyl-3-methyl-5-pyrazolone (PMP) precolumn derivatization method referring to Wang *et al.*[19] The mobile phase was ammonium acetate (0.1 M) and acetonitrile (83 : 17, v/v), the flow rate was 1 mL min^{-1}, the column temperature was 30 °C and the UV absorption wavelength was 250 nm.

2.6 *In vitro* antioxidant activity analysis

APS solutions were prepared with concentrations of 0.06, 0.125, 0.25, 0.5, 1, 2, 4, and 8 mg mL^{-1}. The hydroxyl, DPPH and ABTS radicals scavenging abilities of APS were determined according to a reported method,[20] and the absorbance values were measured using Multiskan SkyHigh Plate reader with deionized water as the blank control.[21] The percentage of scavenging activity was calculated according to eqn (3). The reducing power of APS was measured according to the previous method,[22] and expressed in Trolox equivalent and normalized.

$$\text{Scavenging activity } (\%) = \left(1 - \frac{A_i - A_j}{A_k}\right) \times 100 \quad (3)$$

where A_i, A_j and A_k are the absorbance values of the sample, background control of sample and blank control, respectively.

2.7 Statistical analysis

All experiments are performed in triplicate, and all data are shown as the mean ± standard deviation (SD). One-way analysis of variance (ANOVA) is conducted using GraphPad Prism 7.0, IBM SPSS Statistics 25.0 and Origin 2018 software. Significant differences were set at $P < 0.05$.

3. Results and discussion

3.1 Single factor analysis

3.1.1 Influence of resin amount on the decolorization efficiency. When the resin amount was in the range of 0.5–1.5 g, the decolorization ratio significantly ($P < 0.05$) increased with the increase of resin amount and then stabilized (Fig. 2A). However, when the amount of resin increased to over 1.5 g, the

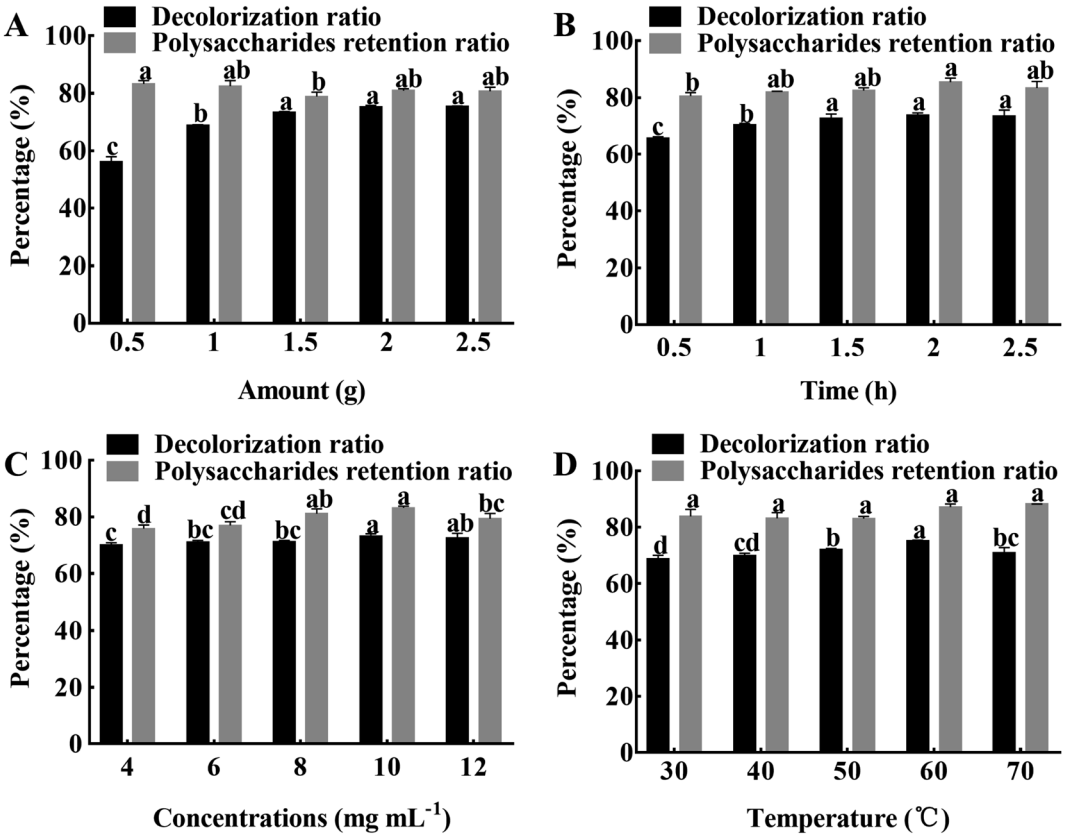

Fig. 2 The effects of different decolorization conditions. (A) Amount of resin. (B) Adsorption time. (C) APS concentrations. (D) Adsorption temperature. The results were expressed as mean value ± SD ($n = 3$). Different letters mean that there are significant ($P < 0.05$) differences in different levels in the same group.

decolorization ratio and retention ratio of the polysaccharides did not significantly change. The reason may be that when the amount of resin increases, the surface area in contact with the solvent increases, prompting the pigment molecules to be better absorbed.[7] After comprehensive consideration, the optimal amount of resin was determined to be 1.5 g.

3.1.2 Influence of adsorption time on the decolorization efficiency. The decolorization ratio significantly ($P < 0.05$) increased during the early stage of adsorption and reached a maximum of 73.90% at 2 h of adsorption (Fig. 2B). It may be that the pigment molecules have the same polarity as the resin, driving the rapid adsorption. The polysaccharides retention ratio increased gradually with increasing adsorption time and then tended to equilibrate; when the adsorption time was 2 h, the retention ratio reached a maximum of 85.35%. It is possible that the amount of pigment molecules and polysaccharides adsorbed by the resin reached saturation with the passage of time.[18] There is no significant difference in the decolorization ratio of polysaccharides, and the retention ratio is higher at 2 h, therefore, an adsorption time of 2 h was chosen as the optimal condition.

3.1.3 Influence of polysaccharides concentrations on the decolorization efficiency. The effects of polysaccharides concentration on decolorization ratio and retention ratio are shown in Fig. 2C. The decolorization ratio significantly ($P < 0.05$) increased with increasing concentration within 4 to 10 mg mL^{-1}, and then gradually decreased as the concentration further increased. At the same time, the polysaccharides retention ratio also followed the same trend. It may be that the adsorption capacity of the resin becomes saturated due to the high concentration of polysaccharides.[23] After comprehensive consideration, the polysaccharides concentration of 10 mg mL^{-1} was chosen for the follow-up experiment.

3.1.4 Influence of adsorption temperature on the decolorization efficiency. The effects of adsorption temperature on decolorization ratio and retention ratio are shown in Fig. 2D. When the temperature was in the range of 30–70 °C, the decolorization ratio of polysaccharides showed a trend of significant ($P < 0.05$) increase at first and then stabilize, and when the temperature was 60 °C, the decolorization ratio reached the maximum of 75.22%. While the change of polysaccharides retention ratio was not significant in the range of 30–70 °C. With the increase of temperature, the activity of pigment molecules increases, and it is more likely for the pigment molecules to reach the resin surface, resulting in a higher decolorization efficiency.[18] Therefore, the adsorption temperature of 60 °C was selected for the next experiment.

3.2 Response surface experiment optimization

3.2.1 Regression modeling. The decolorization efficiency is shown in Table 2. The results were analyzed by multiple

Table 2 Response values for the decolorization ratio in the Box–Behnken design

No.	*A*	*B*	*C*	Decolorization ratio (%)
1	1	0	1	70.53 ± 0.34
2	1	0	−1	68.00 ± 0.36
3	0	0	0	74.99 ± 0.51
4	0	−1	1	60.14 ± 0.14
5	0	1	−1	57.99 ± 0.24
6	1	1	0	73.53 ± 0.29
7	−1	1	0	70.89 ± 0.27
8	0	0	0	74.91 ± 0.28
9	0	0	0	76.23 ± 0.25
10	0	1	1	71.43 ± 0.23
11	0	0	0	75.96 ± 0.22
12	−1	−1	0	70.36 ± 0.18
13	−1	0	−1	65.51 ± 0.18
14	−1	0	1	68.61 ± 0.35
15	0	0	0	75.58 ± 0.23
16	1	−1	0	73.16 ± 0.16
17	0	−1	−1	67.78 ± 0.34

regression, and the regression equation was expressed as follows:

$$Y = 75.53 + 1.38A + 0.4474B + 1.43C - 0.3374AB - 0.1421AC + 5.27BC - 0.0066A^2 - 3.84B^2 - 7.36C^2.$$

The results of ANOVA are shown in Table 3. The coefficient of determination (R^2) of the model was 0.9956, and $R_{adj}{}^2$ (0.9899) was close to $R_{pred}{}^2$ (0.9724), which implied that the model fitting degree was good. In addition, the *F* value for the model was 175.41 ($P < 0.01$), and the lack of fit of the *F* value was 0.6272, which confirmed the significance and effectiveness of the model. In addition, the *F* values of the independent variables *A*, *B* and *C* were 53.37, 5.62, and 57.38, respectively, indicating that the effects of these variables on the decolorization effect were adsorption time (*B*) < amount of resin (*A*) < adsorption temperature (*C*).[24] The coefficient of variation (CV) is a measure of the percentage of the standard deviation to the mean; the smaller the value is, the better the reproducibility.[25] The CV value in this experiment was 0.76%, which further confirmed the accuracy and reliability of the experimental results. At the same time, Table 3 shows that the independent variables (*A*, *B*, *C*), the interaction terms (*BC*) and quadratic terms (B^2, C^2) had significant ($P < 0.05$) effects on the decolorization ratio. All these statistics indicated the reliability of the models.

Table 3 Analysis of variance for the Box–Behnken design experiment[a]

Source	SS	DF	MS	*F*-Value	*P*-Value	Significance
Model	450.09	9	50.01	175.41	<0.0001	**
A	15.22	1	15.22	53.37	0.0002	**
B	1.60	1	1.60	5.62	0.0496	*
C	16.36	1	16.36	57.38	0.0001	**
AB	0.4553	1	0.4553	1.60	0.2468	
AC	0.0807	1	0.0807	0.2831	0.6111	
BC	111.05	1	111.05	389.51	<0.0001	**
A^2	0.0002	1	0.0002	0.0006	0.9804	
B^2	62.00	1	62.00	217.46	<0.0001	**
C^2	228.28	1	228.28	800.68	<0.0001	**
Residual	2.00	7	0.2851			
Lack of fit	0.6486	3	0.2162	0.6419	0.6272	
Pure error	1.35	4	0.3368			
Cor total	452.09	16				

[a] $R^2 = 0.9956$, $R_{adj}{}^2 = 0.9899$, ** is very significant ($P < 0.01$), * is significant ($P < 0.05$).

3.2.2 Interaction analysis. Two-dimensional (2D) contour plots and three-dimensional (3D) response surface plots were used to visually depict the regression equations. A dense and elliptical shape of the contour plot, or a larger slope of the response surface plot, indicated a more significant interaction. 2D contour and 3D response surface analysis indicated that the predicted maximum response value of the dependent variable was located at the smallest ellipse of the contour plots or the peak of the response surface plots.[26] Fig. 3A–D showed the response surface and contour plots for the interaction of amount (*A*) with time (*B*) and amount (*A*) with temperature (*C*), respectively. However, the sparse contour plots and smooth surfaces indicated that the interaction between the various of variables was not significant. Fig. 3E and F were the response surface and contour plots of the interaction between time and temperature. It could be seen that the response surface plots had a downward opening and the highest point, as well as the contour plots was dense and elliptic, which indicated that the interaction between temperature and time was significant ($P < 0.01$).

3.2.3 Model validation. From the response surface analysis, the theoretical optimal prediction conditions for APS decolorization were 1.418 g of resin amount, an adsorption time of 1.924 h and an adsorption temperature of 57.918 °C, and the value of the theoretical decolorization ratio was 71.038%. Combined with the feasibility and convenience of the actual operation, the optimal process parameters were slightly adjusted to the resin amount of 1.4 g, adsorption time of 2 h, and adsorption temperature of 58 °C. The decolorization ratio obtained from the experiment was 71.43 ± 0.23%, which was relatively consistent with the predicted value, indicating that the response surface test and regression equation were accurate and reliable in the APS decolorization analysis.[26]

3.3 Adsorption kinetics analysis

Pseudo-first-order, pseudo-second-order, Elovich and intra-particle diffusion models were used to study the adsorption kinetic curve of pigment molecules in the APS solution by an S-8 macroporous adsorption resin to explore the adsorption mechanism of the S-8 macroporous adsorption resin on the APS pigment molecules.

The pseudo-first-order equation can be expressed as follows:

$$\ln(q_e - q_t) = \ln q_e - k_1 t \quad (4)$$

Pseudo-second-order kinetic reactions are determined by two factors,[27] which is expressed as follows:

$$t/q_t = 1/(k_2 q_e{}^2) + t/q_e \quad (5)$$

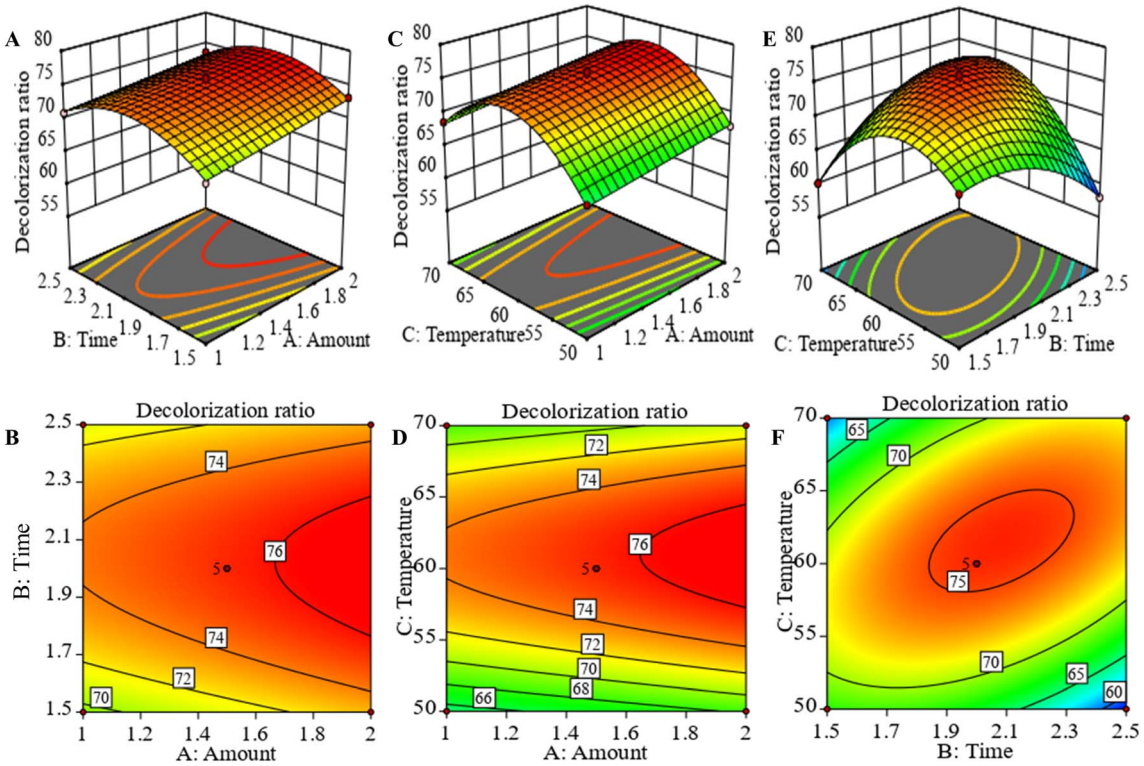

Fig. 3 Response surface and contour plots of the decolorization ratio of APS. Amount of resin and time (A and B). Amount of resin and temperature (C and D). Time and temperature (E and F).

where t (min) represents time; q_e (g^{-1}) and q_t (g^{-1}) represent the adsorption capacity of the resin at equilibrium and at different times, respectively; k_1 and k_2 represent the rate constants of pseudo-first-order and pseudo-second-order reactions, respectively.

The chemisorption dynamics of solid–liquid systems are usually studied using the Evolich model, which is expressed as follows:

$$q_t = 1/b \times \ln(ab) + 1/b \times \ln(t) \quad (6)$$

where a represents the initial adsorption rate and b represents the desorption constant.

The adsorption reaction mechanism could be revealed by the internal diffusion model, whose expression is:

$$q_t = K_3 t^{1/2} + A \quad (7)$$

where K_3 represents the internal diffusion rate constant and A represents proportion to the thickness of the boundary layer constant.

The kinetic curves of the APS pigment molecules in the resin at different temperatures are shown in Fig. 4A. The higher the temperature was, the higher initial adsorption rate and the shorter time required to reach adsorption equilibrium. At the three temperatures (293 K, 303 K, 313 K), the quantity of APS pigment molecules adsorbed by the S-8 macroporous adsorption resin increased with increasing adsorption time, and the adsorption rate was higher in the first 40 min, then stabilized and reached equilibrium after 90 min. In the early adsorption stage, the concentration difference between the resin surface and the pigment molecules was large, and thus, the adsorption is faster. With the progress of adsorption, the concentration gradient decreases and the number of effective adsorption points decreases, leading to a lower adsorption rate of adsorption.[28] The pseudo-first-order, pseudo-second-order, Elovich and intraparticle diffusion models for the adsorption of pigment molecules in the APS solution by the S-8 macroporous adsorption resin at different temperatures are presented in Fig. 4B–E, and the model constant values are shown in Tables 4 and 5. Among the four models, the pseudo-second-order kinetic model had the highest coefficient of determination at each temperature (R^2 > 0.998). Furthermore, the equilibrium adsorption capacity ($q_{e,cal}$) calculated according to the model was closer to the equilibrium adsorption capacity ($q_{e,exp}$) obtained from the experiment, which indicated that it could better fit the adsorption kinetic process of APS pigment molecules by the S-8 macroporous adsorption resin.

As shown in Table 5, when the temperature increased, the initial adsorption rate constant of the Elovich model increased, which indicated that increasing the temperature could improve the initial reaction rate. Moreover, the coefficient of determination of the Elovich model was superior to the internal diffusion model, indicating that the adsorption of APS pigment molecules by the S-8 macroporous adsorption resin was the result of the interaction of the reaction rate and external diffusion.[18,29]

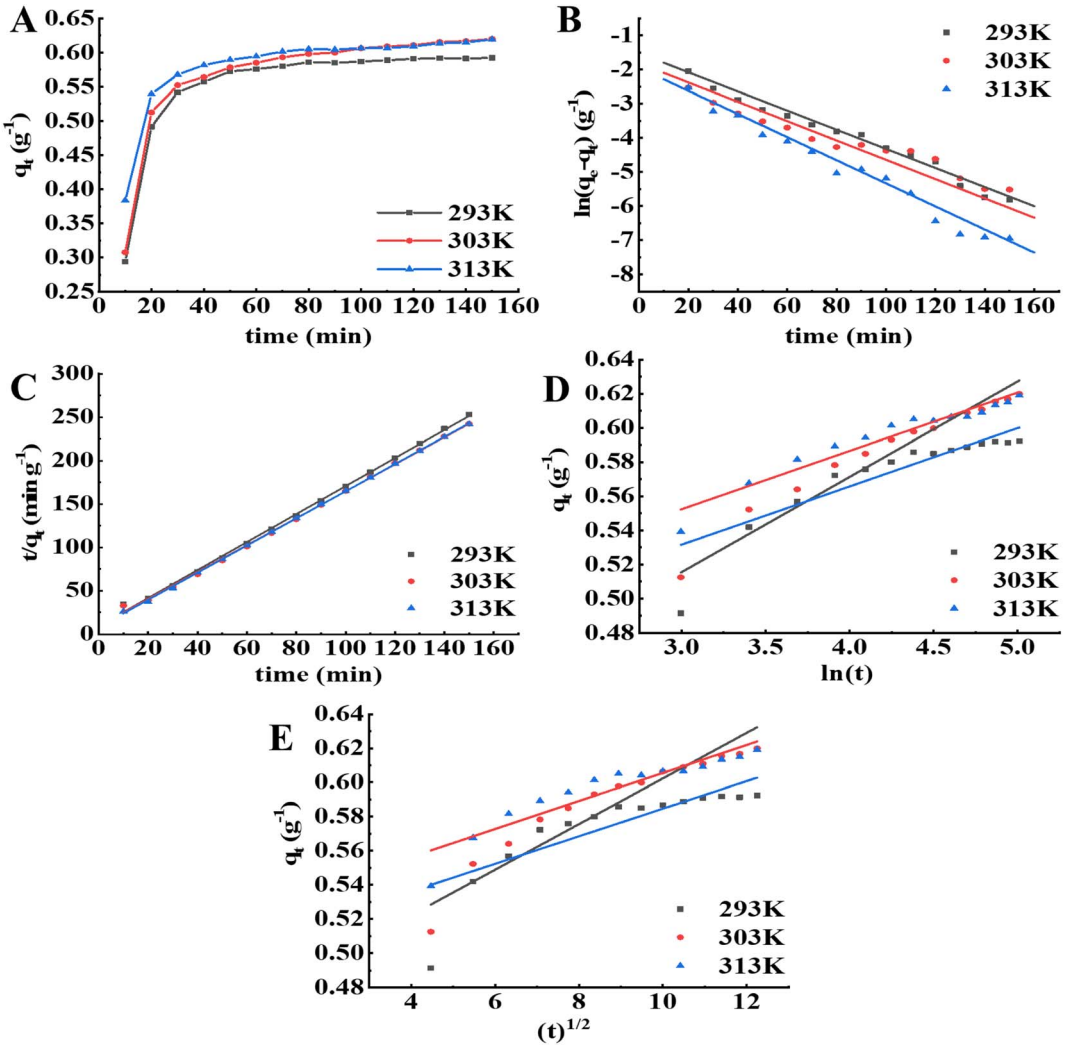

Fig. 4 Adsorption kinetics analysis of the resin on pigment molecules in APS at different temperatures. (A) Adsorption kinetic curves. (B) Pseudo-first-order model. (C) Pseudo-second-order model. (D) Evolich model. (E) Intraparticle diffusion model.

The adsorption of pigment molecules on a macroporous adsorbent resin is a continuous process that includes external diffusion, membrane diffusion, internal diffusion and adsorption. When there was internal diffusion in the adsorption process, the fitting result of q_t *versus* $t^{1/2}$ in the model was linear, and when the fitting line crossed the origin, the adsorption rate was mainly determined by intraparticle diffusion. Fig. 4E shows that the fitted line did not cross the origin, indicating that the adsorption rate was not only singularly influenced by intraparticle diffusion,[30,31] but also affected by other processes, such as boundary layer control, which might also affect the adsorption of pigment molecules.[32] Moreover, the relatively small R^2 value for intraparticle diffusion may be related to the fact that the adsorption mechanism of the resin on the APS pigment molecules is controlled by multiple diffusion processes.

Table 4 Pseudo-first-order and pseudo-second-order model parameters at different temperatures

		Pseudo-first-order			Pseudo-second-order		
T (K)	$q_{e,exp}$ (g^{-1})	$q_{e,cal}$ (g^{-1})	k_1	R^2	$q_{e,cal}$ (g^{-1})	k_2	R^2
293	0.6199	0.2187	0.0280	0.9550[a]	0.6495	0.2108	0.9991[a]
303	0.6191	0.1634	0.0283	0.8893[a]	0.6345	0.3665	0.9997[a]
313	0.5922	0.1428	0.0339	0.8206[a]	0.6123	0.3511	0.9989[a]

[a] Significance at $P < 0.01$ probability level.

Table 5 Elovich and intraparticle diffusion model parameters at different temperatures

	Elovich			Intra-particle diffusion		
T (K)	a	b	R^2	K_3	A	R^2
293	28.5193	17.9211	0.9297[a]	0.0134	0.4587	0.8480[a]
303	18 165.9467	29.2997	0.9360[a]	0.0082	0.5235	0.8600[a]
313	18 171.2803	29.2911	0.8816[a]	0.0081	0.5039	0.7849[a]

[a] Significance at $P < 0.01$ probability level.

3.4 Adsorption isotherm analysis

To investigate the adsorption isotherm of pigment molecules in an APS solution by an S-8 macroporous adsorption resin, the experimental results were fitted by the Langmuir, Freundlich and Temkin models to calculate the maximum adsorption capacity.[33,34] The Langmuir model is suitable for monolayer adsorption on homogeneous surfaces;[18] the Freundlich isothermal adsorption depends on the interaction of adsorbent molecules, making it suitable for nonlinear multilayer adsorption on nonuniform surfaces;[35] and the Temkin isotherm model assumes that the heat of adsorption decreases linearly with increasing contact area.[36] The linearized forms of the Langmuir, Freundlich and Temkin isotherm equations are, respectively:

$$C_e/q_e = C_e/q_m + 1/(K_4 q_m) \quad (8)$$

$$\ln q_e = \ln K_5 + \ln C_e/n \quad (9)$$

$$q_e = RT/f_1 \times \ln B + RT/f_1 \times \ln C_e \quad (10)$$

where q_e (g^{-1}) and q_m (g^{-1}) represent the adsorption capacity of the equilibrium and the theoretical saturation, respectively; C_e represents the equilibrium concentration; K_4 represents the adsorption equilibrium constant; K_5, n, f_1 (J mol^{-1}) and B represent constants; T (K) represents the temperature in Kelvin; and R (J mol^{-1} K^{-1}) represents the gas constant, 8.314.

The adsorption properties of the S-8 macroporous adsorption resin on APS pigment molecules at different temperatures (293 K, 303 K, 313 K) were investigated. As illustrated in Fig. 5A, qe gradually increased with increasing temperature, indicating that the adsorption reaction in this study was endothermic and that warming was beneficial to the adsorption of pigment molecules on the resin.[18] Warming temperature increases the kinetic energy of the molecules and affects the diffusion rate of pigment molecules through the outer boundary layer and in the pores of adsorbent,[30,31] which in turn affects the migration rate. At the same time, more adsorption sites will be generated on the resin surface, which is conducive to adsorption.[36] Similarly, the q_m values of the Langmuir isotherm, the K_5 values of the Freundlich isotherm, and the b_1 values of the Freundlich

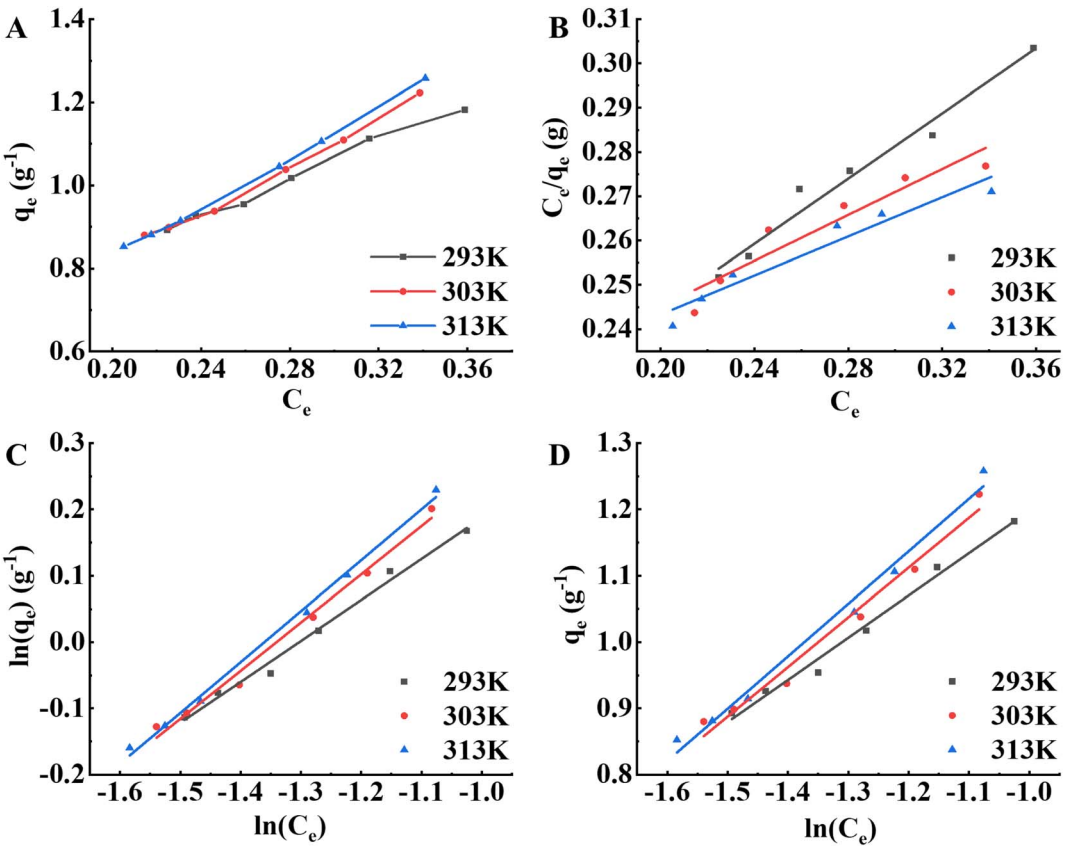

Fig. 5 Adsorption isotherm analysis of the S-8 macroporous adsorption resin on pigment molecules in APS at different temperatures. (A) Adsorption isotherm curves. (B) Langmuir isotherm model. (C) Freundlich isotherm model. (D) Temkin isotherm model.

isotherm increased with warming temperature, as shown in Fig. 5B–D, which also confirmed this conclusion, while all n values were higher than 1 in the Freundlich isotherm, indicating that the resin had a better adsorption capacity for pigment molecules during the study.[18] Table 6 shows that the Freundlich isotherm model had the highest determination coefficient; that is, the Freundlich model was more accurate in predicting the adsorption capacity of pigment molecules adsorbed by the S-8 macroporous adsorption resin.

3.5 Thermodynamic analysis of adsorption

According to the above experiments, the Freundlich model was more accurate in predicting the adsorption process. The expressions of enthalpy change (ΔH, kJ mol^{-1}), Gibbs free energy change (ΔG, kJ mol^{-1}), and entropy change (ΔS, J mol^{-1} K^{-1}) in the Freundlich model are as follows:

$$\mathrm{d}\ln(C_e)/\mathrm{d}T = -\Delta H/RT^2,\ \ln C_e = \Delta H/RT + C \quad (11)$$

$$\Delta G = -nRT \quad (12)$$

$$\Delta S = (\Delta H - \Delta G)/T \quad (13)$$

where C is a constant; the values of ΔH are calculated from the slope and intercept of $\ln C_e$ *versus* the $1/T$ curve.

The negative ΔG and positive ΔH values in Table 7 indicated that the adsorption of the pigment molecules on the resin was spontaneous and endothermic,[30] which was consistent with the above results. Moreover, the absolute value of ΔG gradually increased with increasing temperature, which also indicated that warming was conducive to adsorption.[31] Since ΔH was positive but below 40 kJ mol^{-1}, the adsorption of APS pigment molecules by the S-8 macroporous adsorption resin was dominated by physical adsorption.[37] Furthermore, $\Delta S > 0$ in the experiment, indicating that the adsorption reaction was an entropy-increasing process with more chaotic molecular motion at the solid–liquid interface,[38] and more water molecules moved randomly from the solid surface to the solution. These thermodynamic parameters suggested that the S-8 macroporous adsorption resin was effective in removing pigments from APS and had the potential to be used as a high-efficiency adsorbent.

3.6 Characterization of APS after decolorization with a resin

The UV spectrum, FT-IR spectrum and monosaccharide composition of APS after decolorization are shown in Fig. 6. The spectrum of the decolorized polysaccharides had no obvious absorption peak across the full wavelength range of 200 to 800 nm (as shown in Fig. 6A), indicating that APS contained almost no pigment.[18] In addition, there were no significant absorption peaks at 260 nm and 280 nm, indicating that APS did not contain nucleic acids and proteins.[39]

The FT-IR spectrum of the decolorized APS is shown in Fig. 6B. The broad and strong signal peak near 3422.94 cm^{-1} was attributed to the stretching vibration of O–H,[40] and the weak absorption peak at 2929.41 cm^{-1} was ascribed to the stretching vibration of C–H.[23] The asymmetric stretching vibration at 1640.48 cm^{-1} indicated the presence of O–C–O bonds and glycosidic linkages.[41] Furthermore, the presence of an absorption peak at 1424.31 cm^{-1} indicated that APS contained uronic acid. The characteristic absorption peak at 1037.62 cm^{-1} was caused by the vibration of C–O–C, indicating that APS contained a pyranose ring.[42] The absorption peak near 874.45 cm^{-1} indicated the presence of a β-glycosidic bond, and the absorption peak at 607.23 cm^{-1} proved the skeleton structure of the pyranose in APS.

The monosaccharide composition of APS by comparison with the standard peak times of each monosaccharide is shown in Fig. 6C and D. APS contained mannose (Man), glucose (Glc), galactose (Gal), arabinose (Ara) and glucuronic acid (GlcA), with a molar ratio of 1.18 : 8.04 : 1.22 : 0.92 : 1.

Table 6 Langmuir, Freundlich and Temkin modeling parameters at different temperatures

	Langmuir			Freundlich			Temkin		
T (K)	q_m (g^{-1})	K_4	R^2	K_5	n	R^2	B	f_1 (J mol^{-1})	R^2
293	2.7179	2.1518	0.9720[b]	2.2372	1.6181	0.9901[b]	13.9685	3288.5746	0.9871[b]
303	3.8638	1.3386	0.9023[a]	2.6510	1.5852	0.9889[b]	14.6443	3360.5587	0.9793[b]
313	4.5364	1.1084	0.9365[a]	2.8428	1.5425	0.9962[b]	17.8279	5130.1649	0.9881[b]

[a] Significance at $P < 0.05$ probability level. [b] Significance at $P < 0.01$ probability level.

Table 7 Thermodynamic data for the S-8 macroporous adsorption resin with APS pigments

		ΔG (kJ mol^{-1})			ΔS (J mol^{-1} K^{-1})		
q_e (g^{-1})	ΔH (kJ mol^{-1})	293 K	303 K	313 K	293 K	303 K	313 K
0.1	25.482	−3.942	−3.993	−4.014	100.423	97.277	94.236
0.2	17.179				72.085	69.875	67.709
0.3	12.309				55.464	53.802	52.150
0.4	8.834				43.604	42.333	41.479

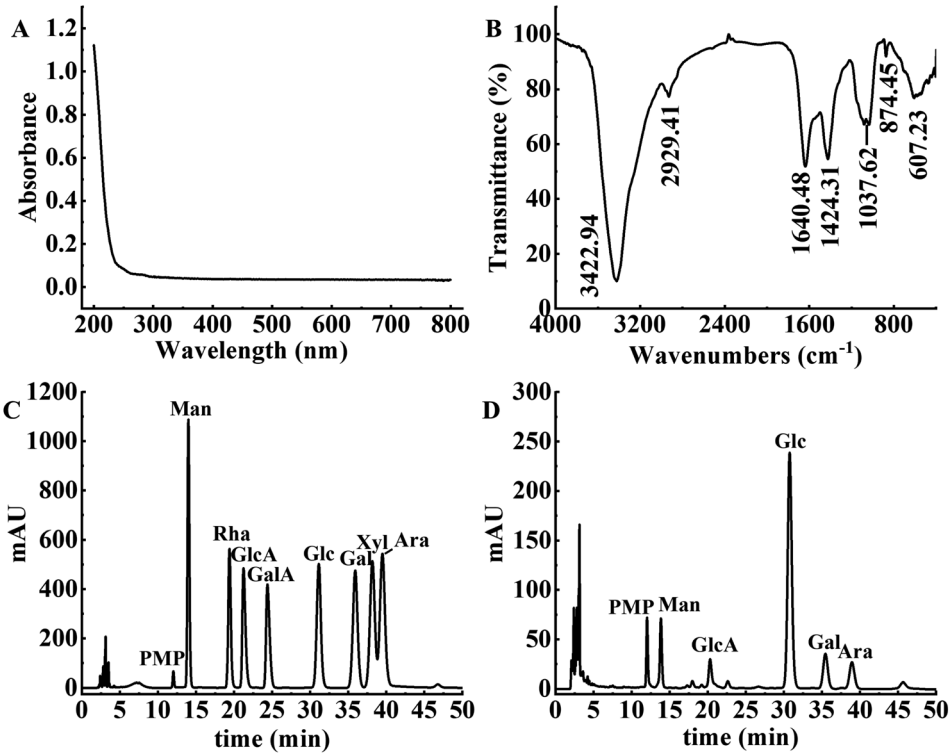

Fig. 6 Structural characteristics of APS. (A) UV-vis spectra of APS. (B) FT-IR spectra of APS. (C) HPLC chromatography of monosaccharide standards. (D) HPLC chromatography of APS.

3.7 Antioxidant activities of APS *in vitro*

3.7.1 Scavenging activity on hydroxyl radical. Hydroxyl radical easily causes oxidative damage to intact cells and can react with most intracellular biomolecules, causing tissue damage and even cell death.[43–45] Therefore, the elimination of hydroxyl radical is essential to protect living systems. The scavenging ability of APS and Vc on hydroxyl radicals increased with increasing solution concentration (shown in Fig. 7A). The scavenging ability of Vc on hydroxyl radical increased significantly ($P < 0.05$) at first, and reached the maximum when the concentration was 0.5 mg mL^{-1}. The scavenging effect of APS on hydroxyl radical was not significant when its concentration was below 1 mg mL^{-1}, while its scavenging ability increased significantly ($P < 0.05$) when its concentration was within the range of 1 to 8 mg mL^{-1}. APS may scavenge hydroxyl radical and terminate free radical chain reactions through the interaction between hydrogen and free radicals.[19] The other possibility is that APS can terminate the reaction by binding to ions essential for the free radical chain reaction.[46]

3.7.2 Scavenging activity on DPPH radical. DPPH radical scavenging capacity was achieved by reducing DPPH ultraviolet absorption caused by antioxidants.[47] The scavenging activities of APS and Vc on DPPH radical are illustrated in Fig. 7B. The scavenging effect of Vc on DPPH radical reached 87.25% at a concentration of 0.06 mg mL^{-1}. The scavenging effect of APS on DPPH radical showed a dose-dependent relationship with its concentration, which first increased significantly ($P < 0.05$), and when the concentration of APS was 4.0 mg mL^{-1} the scavenging ability of DPPH radical reached a maximum of 88.53%, indicating that APS had a better scavenging effect on DPPH radical. The scavenging ability of APS for DPPH radical may be related to its structure and physicochemical property, and the free radical chain reactions may terminate through their electronic donation ability to free radicals, which is consistent with the reported results.[48,49]

3.7.3 Scavenging activity on ABTS radical. The ABTS radical scavenging capacity has been widely used to evaluate the total antioxidant capacity of biological samples. The scavenging ability of APS to ABTS radical was dose-dependent compared with Vc (shown in Fig. 7C). When the concentration of APS was below 2 mg mL^{-1}, the ABTS radical scavenging ability was enhanced sharply with increasing concentration ($P < 0.05$), and the ABTS scavenging ability of APS at a concentration of 2 mg mL^{-1} was 99.93%, indicating that APS had good ABTS radical scavenging activity. It is possible that the presence of glyoxylate in the polysaccharides results in higher ABTS radical scavenging.[50] In addition, ultrasound extraction may damage the cell wall and release some substances that affect their antioxidant activity.[51]

3.7.4 Reducing power. Reducing power is the ability of an antioxidant in a sample to provide electrons to reduce Fe^{3+} to Fe^{2+} and is an important indicator of the activity of an antioxidant,[52] which can be converted to Trolox equivalents from the standard curve to indicate the reducing power of the sample. APS also had a certain reducing power, which did not change significantly when its concentration was low, while the reducing power increased significantly ($P < 0.05$) at concentrations in the range of 1 to 8 mg mL^{-1}. However, the reducing capacity of APS

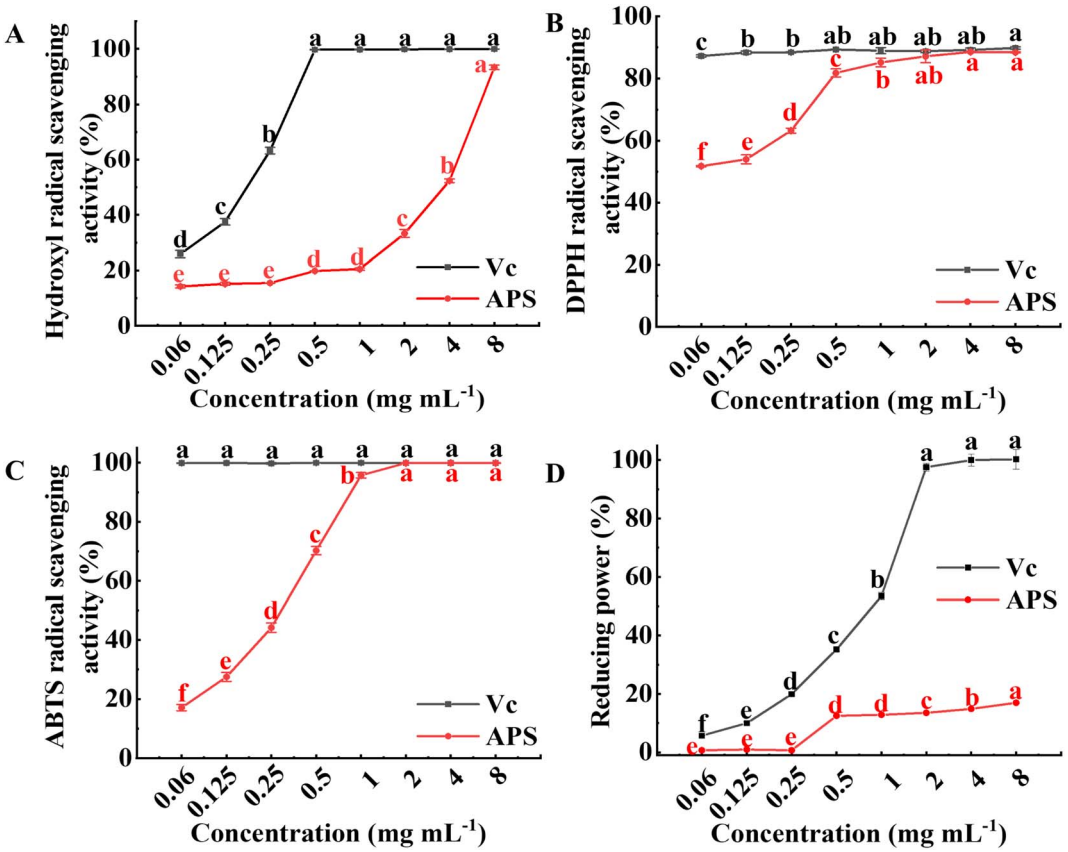

Fig. 7 *In vitro* antioxidant activity of APS. (A) Scavenging activity towards hydroxyl radical. (B) Scavenging activity towards DPPH radical. (C) Scavenging activity towards ABTS radical. (D) Reducing power. The results were expressed as mean value ± SD ($n = 3$). Different letters mean that there are significant differences in different concentrations in the same group ($P < 0.05$).

was lower than that of Vc. The reducing power of polysaccharides may be achieved by breaking down free radical chains, or it may be that polysaccharides can act as effective electron donors to react with free radicals, converting them into stable substances.[53,54]

4. Conclusion

In this study, the decolorization conditions of polysaccharides extracted from alfalfa by S-8 macroporous adsorption resin were optimized through the response surface method, and the physicochemical property and antioxidant activity of decolorized polysaccharides were investigated. The results showed that the S-8 macroporous adsorption resin had a good decolorization effect on the pigment molecules in APS. From the adsorption kinetics and thermodynamic experiments, it was found that the adsorption process of pigment molecules in APS by macroporous adsorption resin was spontaneous and endothermic, and conformed to the pseudo-second-order equation and the Freundlich equation, mainly involving physical adsorption without destroying the structure of the polysaccharides. In addition, this study also revealed that APS had a scavenging capacity for hydroxyl, DPPH and ABTS radicals. In summary, this study provides more insights into understanding the decolorization mechanism of APS, a reliable method for the decolorization process of APS and provides a theoretical basis for further study as a nutraceutical and antioxidant.

Author contributions

Xiaohong Yu: methodology, investigation, formal analysis. Na Mu: methodology, writing – original draft. Xiaochen Liu: software, validation. Yueling Shang: software, formal analysis. Dujun Wang: investigation, writing – review & editing. Fengwei Li: funding acquisition, writing – review & editing.

Conflicts of interest

There are no conflicts to declare.

Acknowledgements

Financial support for this experimental work was provided by the National Natural Science Foundation of China (Grant No. 31802131).

References

1 P. Gao, J. Bian, S. Xu, C. Liu, Y. Sun, G. Zhang, D. Li and X. Liu, *Int. J. Biol. Macromol.*, 2020, **149**, 207–214.

2 X. Liu, S. Xu, X. Ding, D. Yue, J. Bian, X. Zhang, G. Zhang and P. Gao, *Int. J. Biol. Macromol.*, 2020, **147**, 1099–1106.
3 H. Shang, H. Wu, X. Dong, X. Shi, X. Wang and Y. Tian, *Process Biochem.*, 2019, **82**, 179–188.
4 Y. Xie, L. Wang, H. Sun, Y. Wang, Z. Yang, G. Zhang, S. Jiang and W. Yang, *Int. J. Biol. Macromol.*, 2019, **126**, 960–968.
5 Y. Xie, L. Wang, H. Sun, Y. Wang, Z. Yang, G. Zhang and W. Yang, *Int. J. Biol. Macromol.*, 2019, **133**, 1107–1114.
6 L. Chen, M. Ge, Y. Zhu, Y. Song, P. K. Cheung, B. Zhang and L. Liu, *Carbohydr. Polym.*, 2019, **223**, 115076.
7 L. Shao, Y. Sun, J. Liang, M. Li and X. Li, *Int. J. Biol. Macromol.*, 2020, **155**, 1084–1091.
8 F. Lu, R. Zhai, S. Ruan, X. Yang, E. Alenyorege, Y. Wang, Y. Ding and H. Ma, *Lebensm.-Wiss. Technol.*, 2021, **145**, 111384.
9 H. Ren, Z. Li, R. Gao, T. Zhao, D. Luo, Z. Yu, S. Zhang, C. Qi, Y. Wang, H. Qiao, Y. Cui, L. Gan, P. Wang and J. Wang, *Foods*, 2022, **11**, 3449.
10 Y. Zhang, R. Campbell, M. Drake and Q. Zhong, *J. Dairy Sci.*, 2015, **98**, 2982–2991.
11 Y. Shi, T. Liu, Y. Han, X. Zhu, X. Zhao, X. Ma, D. Jiang and Q. Zhang, *Food Chem.*, 2017, **217**, 461–468.
12 Z. Hu, H. Zhou, Y. Li, M. Wu, M. Yu and X. Sun, *Int. J. Biol. Macromol.*, 2019, **132**, 76–86.
13 M. Zhang, F. Wang, R. Liu, X. Tang, Q. Zhang and Z. Zhang, *Lebensm.-Wiss. Technol.*, 2014, **58**, 594–601.
14 J. Sheng and Y. Sun, *Carbohydr. Polym.*, 2014, **108**, 41–45.
15 Z. He, X. Wang, G. Li, Y. Zhao, J. Zhang, C. Niu, L. Zhang, X. Zhang, D. Ying and S. Li, *Int. J. Food Sci. Technol.*, 2015, **50**, 1673–1682.
16 S. Chen, H. Huang and G. Huang, *Int. J. Biol. Macromol.*, 2019, **140**, 1047–1053.
17 S. Kanwal, T. Joseph, L. Owusu, R. Xiaomeng, L. Mei and X. Yi, *Nutrients*, 2018, **10**, 1003.
18 B. Yu, Y. Chen, L. Zhu, M. Ban, L. Yang, Y. Zeng, S. Li, C. Tang, D. Zhang and X. Chen, *RSC Adv.*, 2022, **12**, 3147–3156.
19 K. Wang, J. Guo, J. Cheng, X. Zhao, B. Ma, X. Yang and H. Shao, *Int. J. Biol. Macromol.*, 2021, **191**, 1038–1045.
20 X. Ji, C. Hou, Y. Yan, M. Shi and Y. Liu, *Int. J. Biol. Macromol.*, 2020, **149**, 1008–1018.
21 M. Li, R. Xie, J. Liu, L. Gan and M. Long, *Polym. Degrad. Stab.*, 2020, **182**, 109393.
22 S. Wang, X. Dong and J. Tong, *Int. J. Biol. Macromol.*, 2013, **62**, 387–396.
23 Z. Hu, R. Yu, J. Sun, Y. Duan, H. Zhou, W. Zhou and G. Li, *Process Biochem.*, 2022, **121**, 113–125.
24 X. Gu, L. Zheng, Q. Zhai, J. Sun, H. He, Y. Tang, S. Liang and H. Zhang, *Process Biochem.*, 2022, **121**, 216–227.
25 V. Samavati, *Carbohydr. Polym.*, 2013, **95**, 588–597.
26 X. Liu, Y. Chen, L. Wu, X. Wu, Y. Huang and B. Liu, *Int. J. Biol. Macromol.*, 2017, **103**, 175–181.
27 K. Belaid, S. Kacha, M. Kameche and Z. Derriche, *J. Environ. Chem. Eng.*, 2013, **1**, 496–503.
28 A. Chen and Y. Huang, *J. Hazard. Mater.*, 2010, **177**, 668–675.
29 I. Mall, V. Srivastava and N. Agarwal, *Dyes Pigm.*, 2006, **69**, 210–223.
30 J. Fu, Z. Chen, M. Wang, S. Liu, J. Zhang, J. Zhang, R. Han and Q. Xu, *Chem. Eng. J.*, 2015, **259**, 53–61.
31 X. Ye, L. Wu, M. Zhu, Z. Wang, Z. Huang and M. Wang, *Sep. Purif. Technol.*, 2022, **300**, 121899.
32 S. Wong, N. Ghafar, N. Ngadi, F. Razmi, I. Inuwa, R. Mat and N. Amin, *Sci. Rep.*, 2020, **10**, 2928.
33 X. Jiang, Z. Ouyang, Z. Zhang, C. Yang, X. Li, Z. Dang and P. Wu, *Colloids Surf., A*, 2018, **547**, 64–72.
34 K. Sen and N. Mondal, *Environ. Nanotechnol., Monit. Manage.*, 2021, **16**, 100547.
35 R. Sinha, R. Kumar, K. Abhishek, J. Shang, S. Bhattacharya, S. Sengupta, N. Kumar, R. Singh, J. Mallick, M. Kar and P. Sharma, *Groundw. Sustain. Dev.*, 2022, **18**, 100796.
36 F. Mashkoor and A. Nasar, *J. Mol. Liq.*, 2019, **274**, 315–327.
37 Y. Dong, M. Zhao, D. Waterhouse, M. Zhuang, H. Chen, M. Feng and L. Lin, *Food Chem.*, 2015, **168**, 538–545.
38 Y. Xu, Q. Dang, C. Liu, J. Yan, B. Fan, J. Cai and J. Li, *Colloids Surf., A*, 2015, **482**, 353–364.
39 M. Zhu, R. Huang, P. Wen, Y. Song, B. He, J. Tan, H. Hao and H. Wang, *Carbohydr. Polym.*, 2021, **254**, 117371.
40 X. Ran and H. Yang, *Food Hydrocolloids*, 2022, **133**, 107959.
41 D. Yang, S. Gao and H. Yang, *Food Hydrocolloids*, 2020, **99**, 105317.
42 C. Nie, P. Zhu, S. Ma, M. Wang and Y. Hu, *Carbohydr. Polym.*, 2018, **188**, 236–242.
43 Q. Han, Z. Wu, B. Huang, L. Sun, C. Ding, S. Yuan, Z. Zhang, Y. Chen, C. Hu, L. Zhou, J. Liu, Y. Huang, J. Liao and M. Yuan, *Int. J. Biol. Macromol.*, 2016, **92**, 116–124.
44 L. Huang, M. Shen, X. Zhang, L. Jiang, Q. Song and J. Xie, *Carbohydr. Polym.*, 2018, **200**, 191–199.
45 W. Tang, L. Lin, J. Xie, Z. Wang, H. Wang, Y. Dong, M. Shen and M. Xie, *Carbohydr. Polym.*, 2016, **151**, 305–312.
46 Y. Zhao, W. Hu, H. Zhang, C. Ding, Y. Huang, J. Liao, Z. Zhang, S. Yuan, Y. Chen and M. Yuan, *Int. J. Biol. Macromol.*, 2019, **130**, 238–244.
47 H. Liu, H. Fan, J. Zhang, S. Zhang, W. Zhao, T. Liu and D. Wang, *Food Sci. Hum. Wellness*, 2020, **9**, 71–79.
48 L. Sun, L. Wang, J. Li and H. Liu, *Food Chem.*, 2014, **160**, 1–7.
49 M. Heydarian, H. Jooyandeh, B. Nasehi and M. Noshad, *Int. J. Biol. Macromol.*, 2017, **104**, 287–293.
50 X. Yang, M. Huang, C. Qin, B. Lv, Q. Mao and Z. Liu, *Int. J. Biol. Macromol.*, 2017, **101**, 768–775.
51 M. Shi, Y. Yang, X. Hu and Z. Zhang, *Food Chem.*, 2014, **155**, 50–56.
52 L. Fan, J. Li, K. Deng and L. Ai, *Carbohydr. Polym.*, 2012, **87**, 1849–1854.
53 J. Shi, J. Zhang, Y. Sun, J. Qu, L. Li, C. Prasad and Z. Wei, *Int. J. Biol. Macromol.*, 2016, **91**, 23–30.
54 Y. Ma, D. Zhu, K. Thakur, C. Wang, H. Wang, Y. Ren, J. Zhang and Z. Wei, *Int. J. Biol. Macromol.*, 2018, **111**, 92–101.